QUARTERLY JOURNAL
OF THE
ROYAL METEOROLOGICAL SOCIETY

Vol. 132 APRIL 2006 Part A No. 616

Q. J. R. Meteorol. Soc. (2006), **132**, pp. 691–707 doi: 10.1256/qj.05.126

Simulations of low-level convergence lines over north-eastern Australia

By GERALD L. THOMSEN and ROGER K. SMITH*
Meteorological Institute, University of Munich, Germany

(Received 14 June 2005; revised 16 August 2005)

SUMMARY

We describe high-resolution numerical model simulations of low-level convergence lines over north-eastern Australia using the Pennsylvania State University/National Center for Atmospheric Research Mesoscale Model (MM5). The simulations are for selected events that were documented during the Gulf Lines Experiment, held in September–October 2002. The calculations provide further insights into the dynamics of the convergence lines and the mechanisms involved in their formation. In particular they show two clearly distinct convergence lines, one that corresponds to the morning glory and one which corresponds to the North Australian Cloud Line; the former originates from the east-coast sea breeze over Cape York Peninsula south of about 14°S, while the latter originates from the east-coast sea breeze north of this latitude. They support also a recently proposed conceptual model for the generation of southerly morning glories and show for the first time the separation of a bore-like disturbance following the collision of a nocturnal cold front to the south of the inland trough with a sea-breeze front to the north of the trough. Moreover, they show the progressive transition of the east-coast sea-breeze front and the inland cold front from gravity-current-like flows to bore-like disturbances overnight to form north-easterly and southerly morning glories, respectively.

KEYWORDS: Cloud lines GLEX Mesoscale modelling Morning glory

1. INTRODUCTION

One of the most spectacular atmospheric phenomena in northern Australia is the so-called ‘morning glory’, the name given to a low-level roll-cloud line or a series of such cloud lines that occur early in the morning over the south-eastern part of the Gulf of Carpentaria and adjacent seaboard. The cloud lines are associated with bore-waves that form along a low-level convergence line. The most common cloud lines have a north-west/south-east orientation and move from the north-east. We refer to these as north-easterly morning glories. The convergence line in this case is generated by the sea-breeze circulations over Cape York Peninsula when there is a broad-scale, low-level easterly flow over the peninsula. A closely related phenomenon is the North Australian Cloud Line (NACL), a long line of convective cloud that forms along the west coast of the Cape York Peninsula in the late afternoon or early evening and moves westwards over the gulf during the night and the following day. A comprehensive list of references relating to both phenomena is contained in the review article by Reeder and Smith (1998). It has long been thought that the NACL is associated with the northern extension of the same convergence line that produces the morning glory (see e.g. Smith and Page 1985), but observations during the recent Gulf Lines EXperiment (GLEX)

* Corresponding author: Meteorological Institute, University of Munich, Theresienstrasse 37, 80333 Munich, Germany. e-mail: roger@meteo.physik.uni-muenchen.de

supported, *inter alia*, by calculations presented below suggest that there are two distinct lines. Morning glories are most frequently observed in the late dry season, typically from mid-September until the end of October, although the formation of the low-level convergence line appears to be an almost daily occurrence when there is easterly flow over the peninsula. The NACL is a very common occurrence in these conditions also. During breaks in the wet season, when easterly flow is temporarily re-established over the peninsula and when there is high moisture at low levels, the NACL may develop into a line of thunderstorms. Such events pose a significant forecasting problem in the gulf region.

A second and less common type of morning glory develops overnight to the south of the gulf, or over the gulf itself, and moves northwards, or at least with a significant northward component. The generation of these so-called southerly morning glories is less well understood than that of their north-easterly counterparts, but many appear to be associated with strong ridging to the south of the inland heat trough (Smith *et al.* 1982, 1986). This trough is a climatological feature of the region of north-western Queensland at the times of year when morning glories are most common. Southerly morning glories are discussed also in the review article by Reeder and Smith (1998) and those documented during GLEX will be discussed in a later paper.

A first attempt to determine the predictability of the low-level convergence lines over the gulf is described by Jackson *et al.* (2002) using mesoLAPS, the mesoscale version of the Limited-Area Prediction System (LAPS) of the Australian Bureau of Meteorology (Puri *et al.* 1998). Events were chosen on occasions when cloud lines of various types were clearly visible in satellite imagery and verification was based on the prediction of a low-level convergence line in the observed location and with the observed orientation of the cloud line. Unfortunately, no other data were available for verification. The GLEX experiment was carried out for a period in September–October 2002 in order to remedy the deficiency in the database and to document the occurrence and evolution of the convergence lines in as much detail as possible. To this end, a network of automatic weather stations (AWSs) was installed in the region and an instrumented light aircraft was used to make measurements of lines over the sea. Details of the experiment and the results thereof will be described in further papers.

We describe here some high-resolution numerical model simulations using MM5 of two of the most interesting events documented during the GLEX experiment. We compare these simulations with the data collected during GLEX. Finally, the high-resolution simulations are used as a basis for a detailed study of the convergence lines that produce morning glories and the NACL.

2. The model configuration

The MM5 model is described in detail by Grell *et al.* (1995). In brief, the model is non-hydrostatic and uses a finite-difference approximation to the equations with σ as the vertical coordinate ($\sigma = (p - p_t)/(p_s - p_t)$, where p is pressure, p_s is the surface pressure and p_t the top pressure, which is set to 100 mb). We use 23 σ-levels with 15 levels below 3 km. These have heights of approximately 0, 40, 80, 150, 230, 300, 380, 540, 700, 870, 1200, 1550, 1900, 2300 and 2750 m, giving a relatively high resolution in the boundary layer. The calculations are carried out on the two horizontal domains shown in Fig. 1, an outer domain with relatively coarse resolution and an inner domain with triple this resolution.

In these calculations the outer domain has 221×221 grid points with a horizontal resolution of 9 km and the inner domain has 301×301 points with a horizontal

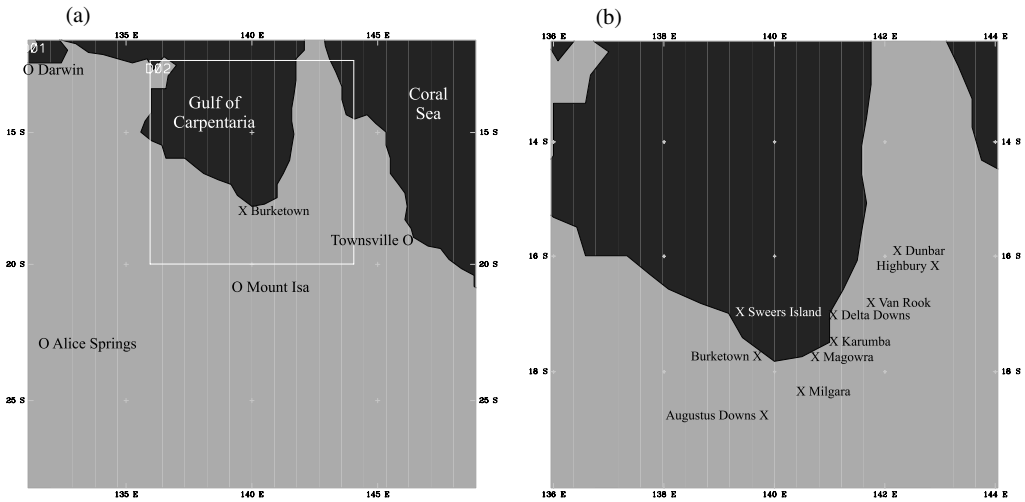

Figure 1. Map of north-eastern Australia showing (a) the coarse domain of the model with places mentioned in the text, and (b) the inner domain with the locations of the automatic weather stations in the southern gulf region marked by crosses.

resolution of 3 km. The terrain land use and topography are taken from the MM5 dataset and have a 5′ resolution for the outer domain and 2′ resolution for the inner domain. The time step is 27 s for the outer domain and 9 s for the inner domain. The Grell cumulus parametrization scheme (Grell 1993) is implemented in the outer domain, but no cumulus scheme is used in the inner domain as the processes believed to be involved in the generation of the morning glory are dry (e.g. Smith and Noonan 1998). The MRF boundary-layer scheme as implemented in the National Centers for Environmental Prediction medium-range forecast system by Hong and Pan (1996) is selected for all domains. In a sensitivity study of all boundary-layer schemes available in MM5, this scheme proved to be most realistic in capturing the GLEX observations. (This study will be the topic for another paper.) The simple Dudhia (1989) scheme is chosen to represent explicit moisture conversions. A short- and long-wave cloud and ground radiation scheme that takes account of diurnal variations is used. Analysis data from the European Centre for Medium Range Weather Forecasts (ECMWF) are used for the initial conditions and boundary conditions. These data have a horizontal resolution of 0.25°. An upper radiation condition is applied to reduce reflection of energy from the model top, preventing spurious noise or energy build-up over topography. The MM5 model has a one-layer bucket soil-moisture model. For this we use soil-moisture data from mesoLAPS, since the ECMWF soil-moisture scheme applies a lower limit which is much too moist for the north Australian dry season and has a deleterious effect on the generation of the sea breezes in the region.

3. TWO MAJOR EVENTS

In this section we focus on two events during the GLEX. All dates and times are given in Eastern Australian Time (EST), which is 10 hours ahead of Universal Time Coordinated (UTC). In the first case, on 4 October 2002, there were three disturbances: a north-easterly morning glory, an NACL and a weak southerly morning glory. In the second case, on 28–29 September 2002, a southerly disturbance moved across the southern half of the gulf. It was composed of two convergence lines; the leading line had

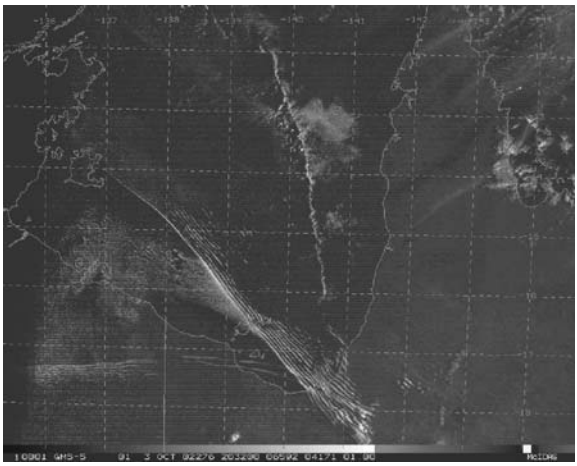

Figure 2. GMS visible image of the Gulf of Carpentaria region at 0630 EST on 4 October 2002.

an undular-bore-like structure and was followed some hours later by a significant air-mass change. In each case we begin by examining the ability of the model to reproduce the observations, including satellite data and data from the AWSs at Augustus Downs, Burketown, Delta Downs, Dunbar, Highbury, Karumba, Magowra, Milgara, Sweers Island and Van Rook, the locations of which are shown in Fig. 1(b). Thereafter we use the model simulations to explore important aspects of the evolution of the convergence lines.

(*a*) *The north-easterly morning glory of 4 October 2002*

Figure 2 shows the Japanese Geostationary Meteorological Satellite (GMS) image for the gulf region at 0630 EST on 4 October 2002. The series of cloud lines stretching north-westwards from the south-eastern corner of the gulf are associated with a north-easterly morning glory, while a line stretching north-north-westwards from the same corner is an NACL. A pair of cloud lines south of the southern gulf coast that form a slightly curved arc oriented approximately east–west is associated with a southerly morning glory.

For this event the calculation commenced at 1000 EST on 3 October. For comparison with Fig. 2, we plot in Fig. 3 the predicted low-level divergence at 0730 EST. A prominent feature of this figure is the convergence line over the southern part of the gulf that corresponds approximately to the observed position of the north-easterly morning glory. The presumption made by Jackson *et al.* (2002) that the cloud lines correspond to lines of enhanced convergence in the low-level divergence patterns was confirmed in the GLEX cases by the surface measurements. The orientation of this convergence line in the calculations corresponds very well to observations (see Table 1). Clearly the model captures the orientation and position of the NACL well.

We examine now the ability of the model to reproduce the surface observations at Karumba and to capture the timing of the morning-glory convergence line at AWSs in the southern part of the gulf. Figures 4(a) and (b) compare observed and model-predicted time series of mean-sea-level pressure (MSLP) at Karumba on 3 October. Figure 4(a) shows the total pressure, while Fig. 4b shows a 12-hour segment of the

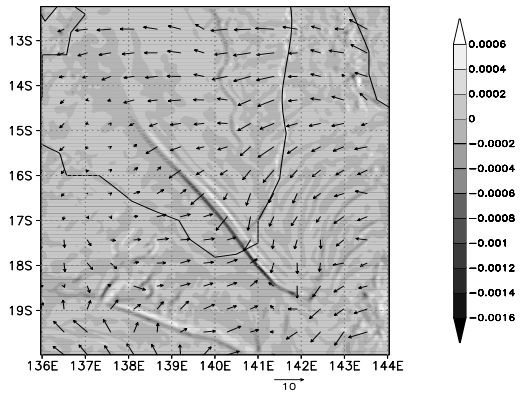

Figure 3. Calculated low-level wind vectors (arrows with scale 10 m s^{-1} below the panel) and divergence (s^{-1}, shading) at level $\sigma = 0.9975$ at 0630 EST on 4 October 2002.

TABLE 1. OBSERVED ORIENTATION OF THE NORTH-EASTERLY MORNING GLORY (NEMG) AND NORTH AUSTRALIAN CLOUD LINE (NACL) IN FIG. 2 COMPARED WITH ORIENTATIONS IN THE MM5 MODEL

	NEMG	NACL
Observed	40°	11°
MM5	40°	9°

The angles are measured anticlockwise from north.

corrected pressure, obtained by first removing the daily trend and then the diurnal and semidiurnal variation. The trend was assumed to be linear throughout the day and the diurnal and semidiurnal variation were removed by performing a Fourier analysis of the pressure and then subtracting the first two wave numbers. The simulation shows a remarkably good agreement with the observed behaviour, but the mean pressure is offset by about 2.5 mb. We attribute this offset to the difference between the mean height of the orography (0 m) in the grid box surrounding Karumba and the actual height of the station there, which was estimated to be 15 m.

Figures 4(c) and 4(d) show time series of the zonal and meridional wind speed at Karumba. The vertical arrows indicate the passage of the morning glory, which is characterized by a sharp change in both wind components. The model captures the time of passage very well, within a few minutes of the observed time.

In an attempt to quantify the overall agreement between the surface pressure observed at AWSs and the corresponding pressures in the model simulation, we calculate the correlation coefficient defined by

$$r = \frac{\sum (p_{\text{obs}} - \overline{p_{\text{obs}}})(p_{\text{mod}} - \overline{p_{\text{mod}}})}{\sqrt{\sum (p_{\text{obs}} - \overline{p_{\text{obs}}})^2 \sum (p_{\text{mod}} - \overline{p_{\text{obs}}})^2}},$$

where the average is taken over the stations listed in Table 2. The subscript 'obs' refers to an observed value and 'mod' refers to a model value. The overlined variables are averaged over the 36-hour integration time. The correlation was found to be $r = 0.95$.

The evolution of the low-level convergence lines in the model is shown in Fig. 5. At 1300 EST the sea breeze has just begun to develop along the west coast of the peninsula and is marked there by a well-defined line of convergence along the coast

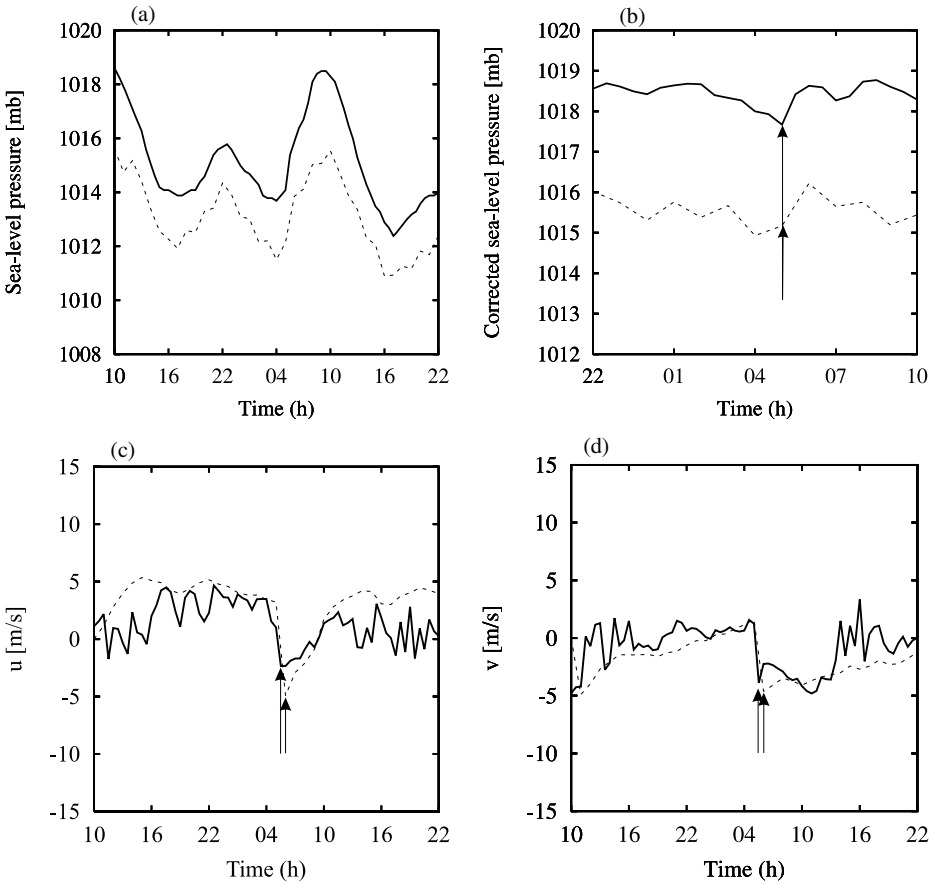

Figure 4. (a) Mean-sea-level pressure, (b) corrected mean-sea-level pressure, (c) zonal wind speed, u, at 10 m and (d) meridional wind speed, v, at 10 m at Karumba on 3–4 October 2002 (times in EST), from measurements (solid) and the MM5 model (dashed). The vertical arrows indicate times of passage of the morning glory.

TABLE 2. OBSERVED TIMES (EST) OF PASSAGE OF THE DISTURBANCE AT AUTOMATIC WEATHER STATIONS COMPARED WITH TIMES INDICATED BY THE MODEL

Station	Observed	MM5
Highbury	2200	0030
Dunbar	2250	0030
Van Rook	0150	0130
Delta Downs	0315	0330
Karumba	0510	0600
Magowra	0540	no signature
Milgara	0620	0700
Sweers Island	0730	0800
Burketown	0845	1000
Augustus Downs	1000	1230

The model output is available only every 30 min.

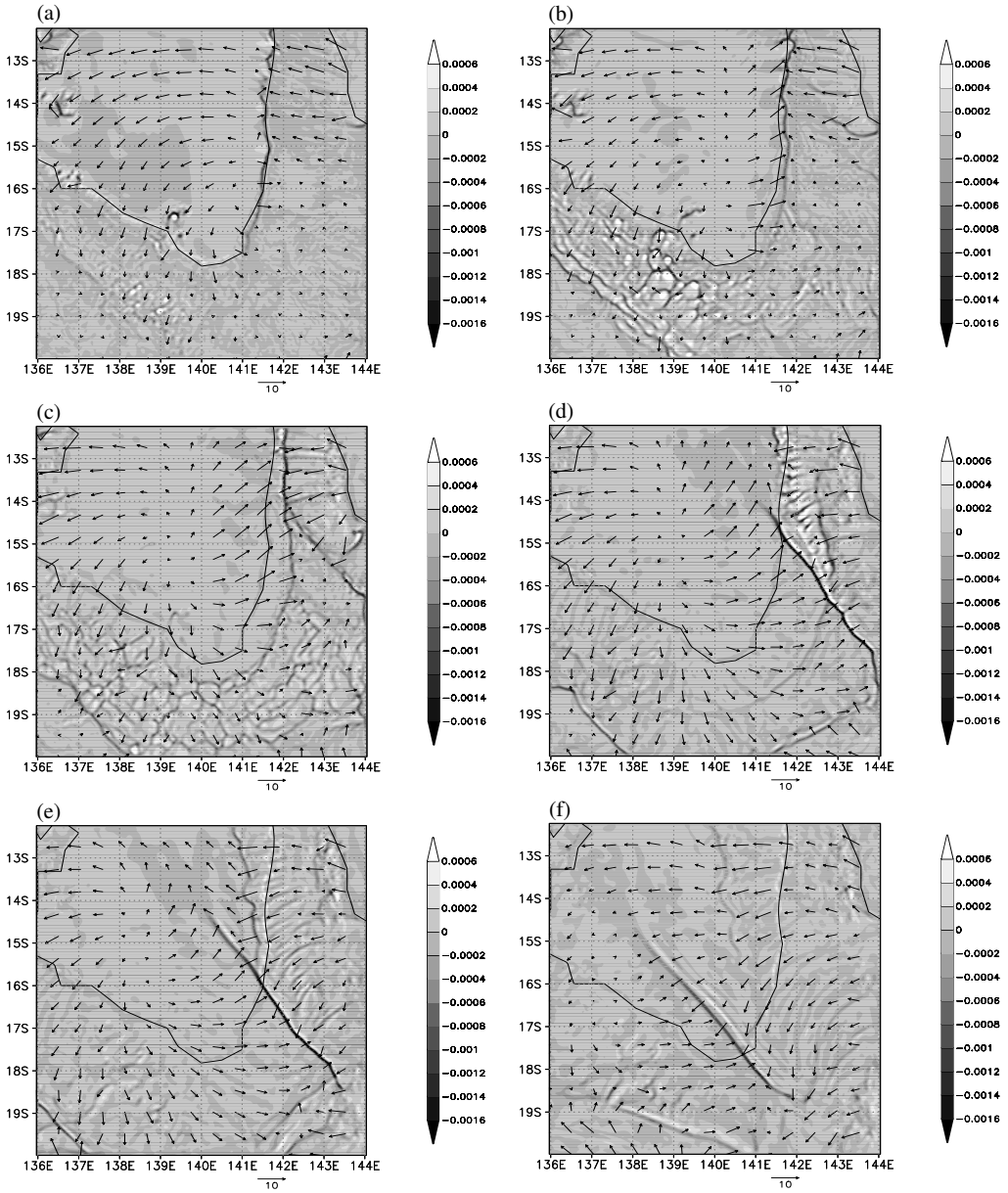

Figure 5. Sequence of plots of wind vectors (arrows, scale 10 m s^{-1} below each panel) and divergence (s^{-1}, shading) at level $\sigma = 0.9975$ from the MM5 run at (a) 1300 EST, (b) 1600 EST, (c) 1900 EST, (d) 2200 EST, (e) 0100 EST and (f) 0630 EST on 3–4 October 2002. The domain size is 900 km × 900 km.

because the broad-scale flow is offshore along this coast. Two short lines of convergence have formed on the north-eastern side of the peninsula as well. There is also a line of convergence approximately parallel to the southern gulf coast and 100 km or more inland and a shorter line nearer to the coast, both west of 140°E. The line further inland is ragged at its south-eastern end suggesting a significant influence of orography in this region.

By 1600 EST the convergence line marking the west-coast sea-breeze front has moved a little inland, especially along its southern part and the lines in the north-east have lengthened. These lines are presumably a result of convergence produced by the onshore acceleration of the easterly flow in conjunction with orography. Note that the daytime occurrence of sharp sea-breeze fronts is favoured by an offshore component of the broad-scale flow (Clarke 1983). At this time, two long coherent lines of convergence are evident south of the gulf, west of 140°E, together with many small cells of convergence, which may be an attempt by the model to capture the largest boundary-layer eddies induced by the irregular terrain in this region.

By 1900 EST, which is close to sunset, the west-coast sea-breeze front has moved further inland and has joined with that which has formed inland of the concave part of the coastline in the south-eastern corner of the gulf. In the north of the peninsula, the three segments of convergence evident in the east at 1600 EST have merged to form a line approximately parallel to the east coast and the collision of the north-western end of this line and the west-coast sea-breeze front has started. There are strong easterly winds to the east of this line in the north and strong north-easterlies further south. This line marks the newly formed east-coast sea-breeze front.

At 2200 EST the east-coast sea-breeze front has become split. North of about 14°S, it is evident as a band of enhanced convergence parallel to the east coast at these latitudes and lying close to the west coast. The line lies offshore north of about 13.5°S and is rather broken south of 13°S. South of 14°S, the line is coherent and almost straight, with its northern end extending out over the gulf. This part of the line is approximately parallel to the east coast of the peninsula south of 14.5°S and has strong north-easterly winds to the north-east and south-westerlies to the south-west. A narrow curved strip of enhanced convergence marks the south-coast and west-coast sea-breeze fronts inland along the entire gulf coastline. This strip intersects the east-coast sea-breeze front at about 16.4°S. Animations of the low-level flow fields show that the convergence lines associated with the sea breezes pass through each other. However, a sequence of vertical–zonal cross-sections of wind and virtual potential temperature at 13°S show that, after the collision, the eastward-moving convergence line propagates as a wave disturbance in the easterly flow and subsequently decays. In the lower right of Fig. 5(d), the south-coast sea-breeze front is already 250 km inland. A second convergence line is also evident a little further inland and separates winds with a northerly or westerly component to the north of it from those with a southerly to easterly component to the south of it. This line is associated with nocturnal ageostrophic convergence into the inland trough.

At 0100 EST on 4 October, the southern section of the east-coast sea-breeze front has moved south-westwards. Behind it over the land are strong north-easterlies, while over the sea the winds behind are south-easterly. At the same time the northern section has regained coherence and forms a separate line of convergence extending south-south-east to north-north-west over the north-eastern part of the gulf. North of its intersection with the east-coast sea-breeze front, the west-coast sea-breeze front has lost its identity. The sea-breeze front from the southern gulf coast has moved further inland, forming an arc near the southern edge of the plotting domain.

Figure 5(f) shows the situation at 0630 EST, the time of the satellite image in Fig. 2. At this time the convergence line that was the east-coast sea-breeze front lies very close to the location of the north-easterly morning glory in the satellite image, which is clear evidence that the latter develops out of the former. Further, the NACL lies close to the convergence line in the northern part of the gulf, the origin of which can be traced back to the east-coast sea breeze along the northern part of the peninsula. An animation of

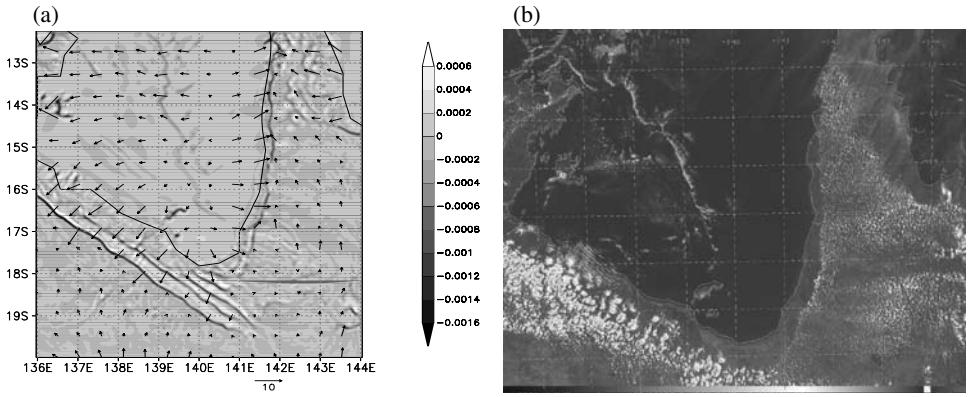

Figure 6. (a) Low-level wind vectors (scale 10 m s^{-1} below panel) and divergence (s^{-1}, shading) for the simulation at $\sigma = 0.9975$ at 1430 EST on 4 October 2002. (b) GMS visible satellite image at 1425 EST on the same day.

the half-hourly fields like those in Fig. 5 shows also a convergence line moving from the south, this being the east–west oriented line at 0630 EST in Fig. 5(f). This line appears to be the attempt of the model to capture the southerly morning glory seen in the satellite image. However, the line is some 150 km too far south of the observed cloud line at its western end and some 200 km at its eastern end. Since the convergence line in the model is still over land when the mixed layer redevelops after sunrise, the line weakens before reaching the southern gulf coast. A likely reason for the incorrect location of this line is its incorrect location in the initial analysis.

Figure 6 compares the satellite picture at 1430 EST on 4 October with model fields like those in Fig. 5. By this time the north-easterly morning-glory cloud line has long moved over land and disappeared in the satellite imagery, but the NACL is still evident. The position of the NACL is tolerably well captured in the model (it is close to 14°S, 139°E in both the model and the image), but the orientation in the model is a little different from that observed. The sea-breeze front along the southern gulf coast and along the west coast of the peninsula is reasonably well captured also. This front is presumably close to the northern/western edge of the cumulus cloud field in the satellite image. An animation of the half-hourly fields like those in Fig. 5 shows that the sea-breeze front along the southern gulf coast forms out of the morning-glory convergence line, which accounts for the series of convergence lines just south of the southern tip of the gulf in the model, although such waves are not seen in the corresponding satellite image. The southern edge of this cloud field, south of the gulf, appears to correspond approximately to a continuous line of enhanced convergence in the model, separating a north-easterly airstream to the north from a south to south-easterly airstream to the south. In the model, this line lies close to (not more than 15 km north of) the mean axis of the inland trough at this time.

The evolution described above provides a modified view of the generation of north-easterly morning glories compared with previous studies. The early idealized calculations by Clarke (1984) and Noonan and Smith (1986, 1987) indicated that the morning glory is generated by the collision of the east- and west-coast sea breezes over the Cape York Peninsula. The collision results in an elevated hump of stably stratified air that subsequently forms a south-westward-propagating bore wave. The observations of bore formation ahead of a cold front over central Australia (Smith *et al.* 1995) and more

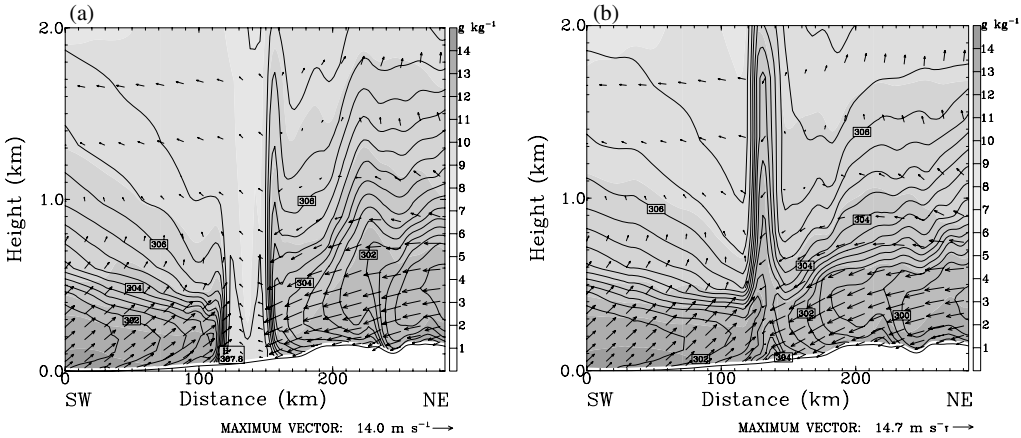

Figure 7. Vertical cross-section of virtual potential temperature (contours, interval 0.5 K), water vapour mixing ratio (g kg^{-1}, shading) and horizontal wind vectors from the surface to 2 km at (a) 1900 EST and (b) 2000 EST on 3 October 2002. The cross-section extends from (15.5°S, 141.5°E) to (13.5°S, 143°E). In (a) the two sea breezes are about to collide and (b) is just after the collision.

recent calculations of morning-glory convergence lines by Smith and Noonan (1998) provide evidence that the collision of the sea breezes is not a necessary prerequisite for producing a bore wave. (In the Smith and Noonan calculations, the convergence line is also well formed south of the gulf coast where no collision occurs.) The foregoing model simulations as well as the more recent mesoLAPS calculations by Jackson *et al.* (2002) all indicate that the morning glory and NACL are associated with the same convergence line, although the observations during GLEX suggested that this is not the case. Indeed, a feature of the foregoing calculation, in contrast to all previous calculations, is the generation of two clearly distinct convergence lines that correspond to the morning glory and to the NACL. The generation mechanism, however, appears to be the same for both lines.

In a very recent study by Goler and Reeder (2004) using an extremely high resolution (200 m in the horizontal) two-dimensional model, the air behind the east-coast sea-breeze front is warmer than the air behind the west-coast sea-breeze front and runs over the west-coast sea breeze to form the morning-glory convergence line. In their calculation the sea surface temperature is the same on both sides of the peninsula. Figure 7 shows a vertical cross-section of virtual potential temperature, θ_v, water vapour mixing ratio and horizontal wind vectors at 1900 EST and 2000 EST on 3 October, shortly before and shortly after the collision of the two sea breezes. Inspection of the 1900 EST cross-section shows that, in the present simulation, the depth of the cold air behind the west-coast sea-breeze front is shallower and the air just behind the front is a little moister than that behind the east-coast sea-breeze front. Furthermore the horizontal gradient of θ_v near the surface is largest across the west-coast sea-breeze front, suggesting that the east-coast sea breeze will rise above the west-coast sea breeze at collision, as in the Goler and Reeder calculations. However, one would not expect the present model with 3 km horizontal resolution to capture the details of the collision process, especially because the boundary-layer scheme that is implemented in the model at all grid points is unlikely to be valid near the collision point. Calculations not shown indicate that the pseudo-equivalent potential temperature of air behind the west-coast sea-breeze front is a little larger than that behind the east-coast sea-breeze front.

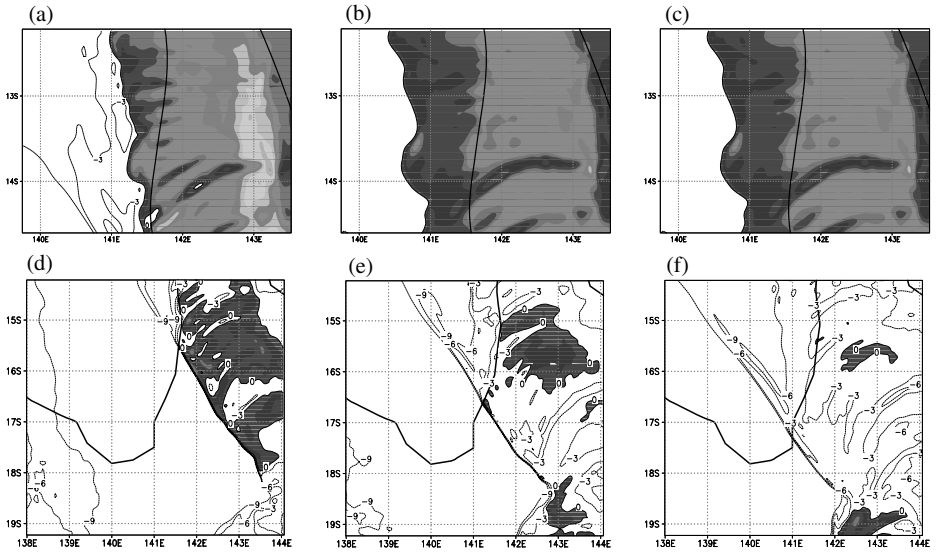

Figure 8. Calculations of the relative flow, $u - c$, normal to and behind the NACL at (a) 0000 EST, (b) 0300 EST and (c) 0500 EST on 4 October 2002 at level $\sigma = 0.965$ in the model run. (d)–(f) are as (a)–(c), but relative to the morning glory. The contour interval is 3 m s^{-1}, with positive values shaded.

Figure 8 shows the relative flow, $u - c$, directly behind the NACL and behind the morning glory at a height of ∼250 m at selected times, where u is the wind speed perpendicular to and towards the line in question and c is the propagation speed of that line. In these calculations, the orientation of the NACL is ∼10° ± 1° at 0000 and 0300 EST on 4 October, and ∼8° ± 1° at 0500 EST, measured anticlockwise from north. The mean propagation speed of this line between 2200 EST on 3 October and 0700 EST on 4 October is ∼4.8 m s^{-1}. The morning-glory line has an orientation of ∼36.7° ± 1° at 0000 EST, ∼39.5° ± 1° at 0300 EST, and ∼40.0° at 0500 EST on 4 October. The translation speeds of this line at these times are 10.1, 10.1 and 10.7 m s^{-1}, respectively. The errors in calculating these propagation speeds are estimated to be less than 1 m s^{-1}. It is seen that the relative flow behind (i.e. to the east of) both lines is positive (i.e. towards the line) after the collision of east- and west-coast sea breezes. A positive value of $u - c$ is indicative of a gravity-current-type flow, while a negative value is characteristic of a bore-like disturbance (Simpson 1997). Figure 8 shows that, for this event at least, the NACL has the clear structure of a gravity current, both before and after the collision of the sea breezes. The same is true of the morning-glory disturbance at first, but $u - c$ progressively declines behind this disturbance and eventually becomes negative. After about 0500 EST, the relative flow behind the morning glory is everywhere negative and its transition to a bore wave is complete.

(*b*) *The southerly morning glory of 28–29 September*

The synoptic situation for this event is exemplified by the MSLP analysis for 2200 EST on 28 September shown in Fig. 9(a). An anticyclone centred in the Great Australian Bight extends a ridge almost to the southern gulf coast, while the inland trough over northern Australia lies just south of this coast. The precursors to this event are seen in the National Oceanic and Atmospheric Administration's Advanced Very High Resolution Radiometer (AVHRR) infrared satellite image at 1950 EST

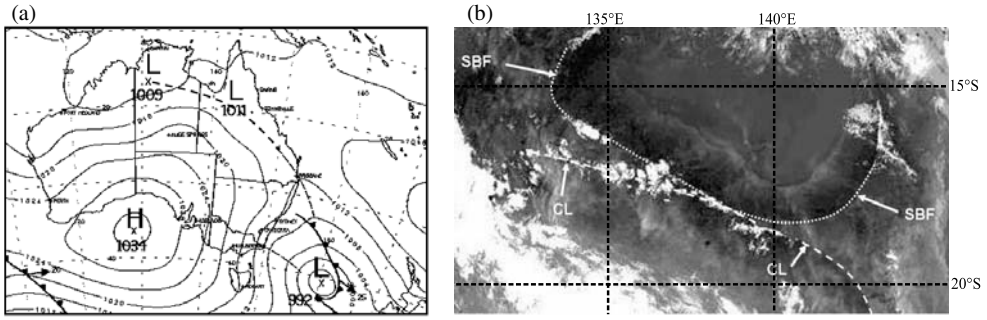

Figure 9. (a) Mean-sea-level pressure at 2200 EST on 28 September 2002 (adapted from Bureau of Meteorology analysis). The inland trough (dashed) lies south of the Gulf of Carpentaria. (b) NOAA AVHRR infrared satellite image for the Gulf of Carpentaria area at 1950 EST on the same day. SBF denotes the sea-breeze front and CL denotes the convergence line.

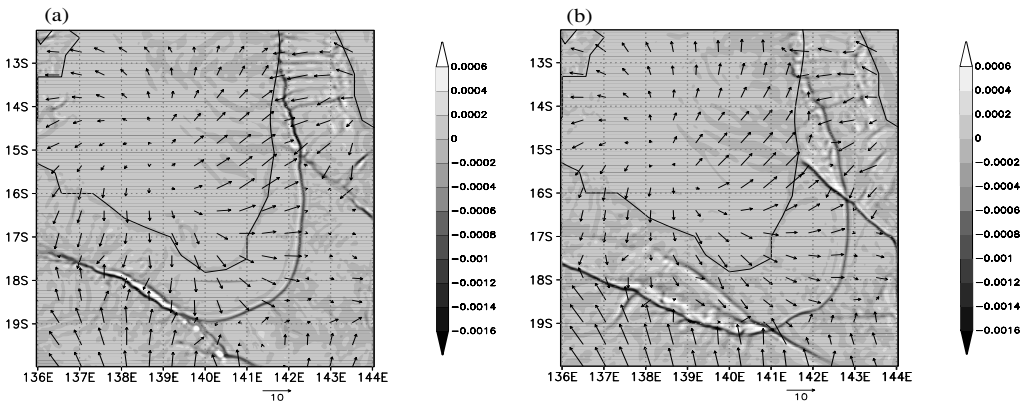

Figure 10. Low-level wind vectors (scale 10 m s^{-1} below each panel) and divergence (s^{-1}, shading) at model level $\sigma = 0.9975$ at (a) 2000 EST and (b) 2200 EST on 28 September 2002. (a) should be compared with the infrared satellite image in Fig. 9(b), which is valid 10 minutes earlier.

on 28 September shown in Fig. 9(b). The image shows the sea-breeze front (dotted in Fig. 9(b)) along the coastal region of the southern and eastern gulf, which is marked partly by line segments of cloud and elsewhere by a sharp gradient in texture, presumably associated with the cooler sea-breeze air. A second boundary evident in Fig. 9(b) is marked also by a sharp gradient in texture and partly by line segments of cloud. This line (dashed in Fig. 9(b)) appears to be associated with a convergence line approaching from the south (see below).

The calculation for this day is initialized at 1000 EST on 28 October. Figure 10 shows the calculated low-level wind and divergence at two times on this day. Figure 10(a) shows the fields at 2000 EST, which should be compared with the satellite image for 1950 EST in Fig. 9(b). It is seen that the position of the sea-breeze front and the convergence line south of it agree well with the positions of these lines in the satellite image (denoted by SBF and CL, respectively). At 2200 EST, the model indicates two separate lines in the southern gulf region, one corresponding to the southerly morning glory in the north and one to the sea breeze in the south. It shows also a north-easterly line oriented south-east/north-west near the west coast of the peninsula,

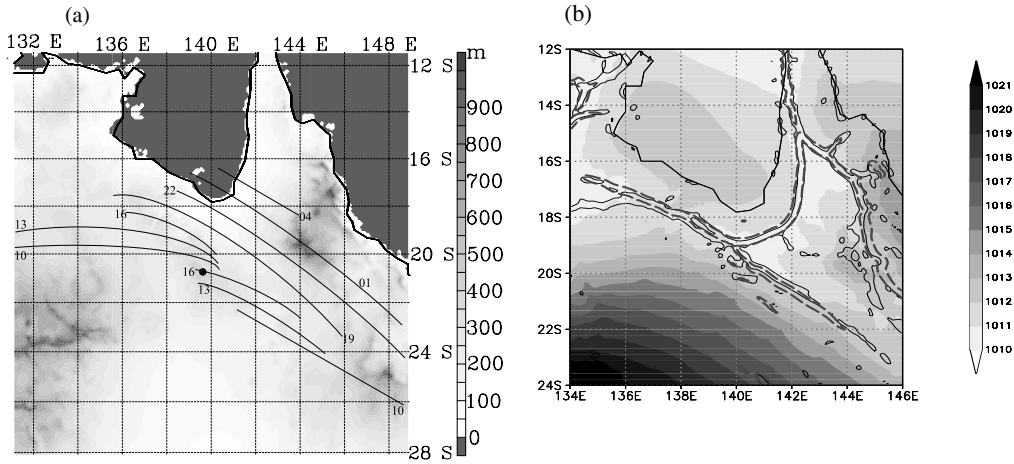

Figure 11. (a) Positions of the trough line (from 1000 to 1900 EST on 28 September 2002) and southerly morning-glory disturbance (from 2200 to 0200 EST on 28–29 September) indicated by thick solid lines. Surface orography is shaded. (b) Mean-sea-level pressure (hPa, shading) at 2000 EST on 28 September, with solid contours showing the regions where the low-level wind divergence is less than -8×10^{-5} s^{-1} (indicating strong convergence), and dashed contours where the water vapour mixing ratio gradient exceeds 8×10^{-4} km^{-1}.

the occurrence of which was evident in the AWS data at Highbury at 2130 EST and Dunbar at 2300 EST. Estimated model times of passage at these stations were 2200 EST and 2230 EST, respectively. The model captures also the west-coast sea-breeze front on the peninsula, the passage of which was observed at Van Rook at 1745 EST and at Dunbar at 1900 EST. The passage times in the model at these stations was 1730 EST and 2000 EST respectively. Taking into account that the model output is available only every half hour, we consider the agreement between the observed and model times to be acceptable. The west-coast sea breeze was not observed at Highbury but, in the model calculation, Highbury was close to the collision point between the east- and west-coast sea breezes.

Figure 11(a) shows isochrones of the northward-moving convergence line(s) in the simulation, while Fig. 11(b) shows the convergence line and the trough line (marked by strong horizontal gradients of water vapour mixing ratio and minimum MSLP) at 2000 EST. The position of the convergence line coincides closely (to within 20 km) with the position of the trough line and with the line marked CL in the satellite image in Fig. 9(b).

Figure 12 shows a vertical cross-section of virtual potential temperature, water-vapour mixing ratio and the (horizontal) wind vectors at 1800 and 2200 EST on 28 September. At 1800 EST the inland trough coincides with the region of warmest air and with the deepest well-mixed layer. The low-level flow to the north-east of the trough is moist and corresponds to the sea breeze from the southern gulf coast. In contrast, the air south-west of the trough is relatively dry and there is a decline in mixed-layer temperature towards the south. (This decline continues much further south than shown in this figure.) Indeed the vertical structure of the atmosphere in this region is reminiscent of that behind a cold front. On the right of Fig. 12(b), the disturbance corresponding to the north-easterly morning glory is evident by the sharp jump in the isentropes.

In an hourly animation of low-level wind divergence and moisture gradient associated with the inland trough, the coherence of the lines is disrupted by the orography in

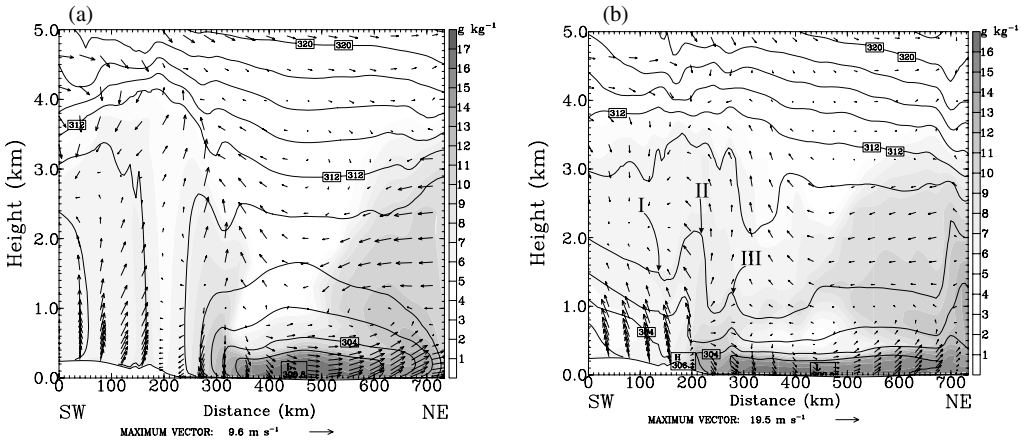

Figure 12. Vertical cross-section of virtual potential temperature (contours, interval 2 K), water vapour mixing ratio (g kg^{-1}, shading) and horizontal wind vectors from the surface to 5 km at (a) 1800 EST and (b) 2200 EST on 28 September 2002. The cross-sections extend from (20°S, 138°E) to (15°S, 142°E), a distance of about 750 km. (The position of the cross-section is indicated by the solid line in Fig. 13(a).) The trough line and sea breeze south of the gulf are shown (a) before their collision near Mount Isa, and (b) after the collision. (b) also shows the disturbance corresponding to the north-easterly morning glory. The Roman numerals refer to positions in Fig. 13(a).

the vicinity of Mount Isa, but becomes re-established as the disturbance moves northwards over the flatter terrain to the north. It is here where it collides with the sea breeze before continuing its generally northward movement. Comparison of the two panels in Fig. 12 shows that, following the collision, the warm dry air between convergence line and sea breeze is raised above the surface and a solitary wave disturbance marked by an elevation of the isentropes is seen ahead of the front at 2200 EST. The latter is the precursor to the model analogue of the southerly morning glory. It has strong southerly winds behind it at low levels.

The disturbance observed on 28–29 September consisted of two convergence lines: a leading line with an undular-bore-like structure followed later by a significant air-mass change. The separation in time between the arrival of each line increased from one and a quarter hours to five hours as the disturbance progressed northwards. The model shows also the formation of two northward-propagating lines. These are seen in Fig. 13, which shows the same fields as Fig. 11, but at 2200 EST on 28 September and 0200 EST on 29 September. By 2200 EST, the convergence line and dry line that were coincident at 2000 EST in Fig. 11(b) have separated (Fig. 13(a)) and the separation continues to 0200 EST (Fig. 13(b)). The leading disturbance associated with the strip of strong convergence labelled SMG in Fig. 13(b) propagates to the north-east, moving ahead of the region of strong moisture gradient. The latter, which marks the dry line, slows down after collision with the sea breeze and the dry air mass arrives at the gulf coast at about 0200 EST on 29 September, comparable with the observed passage at about 0200 EST at Burketown and about 0230 EST at Karumba. Figure 13 shows also the north-easterly disturbance on this day (labelled NEMG in Fig. 13(b)), which was discussed above. While the accuracy of the detailed structures of the convergence lines in the calculation are hard to assess, the broad-scale features of evolution are certainly consistent with the observations.

Figure 14 shows the relative flow in the model, $u - c$, directly behind the two convergence lines (the moving trough line, or dry line, and the bore wave ahead of it)

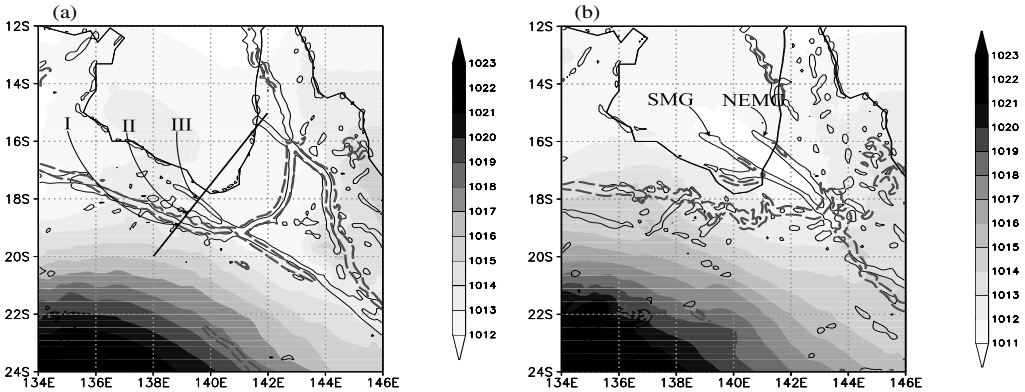

Figure 13. As Fig. 11(b), but for (a) 2200 EST and (b) 0200 EST on 28–29 September. In (a), the solid line indicates the position of the cross-section in Fig. 12(b) and the Roman numerals refer to the positions indicated in that figure. In (b), the leading line of the southerly disturbance and the north-easterly disturbance are denoted SMG and NEMG, respectively.

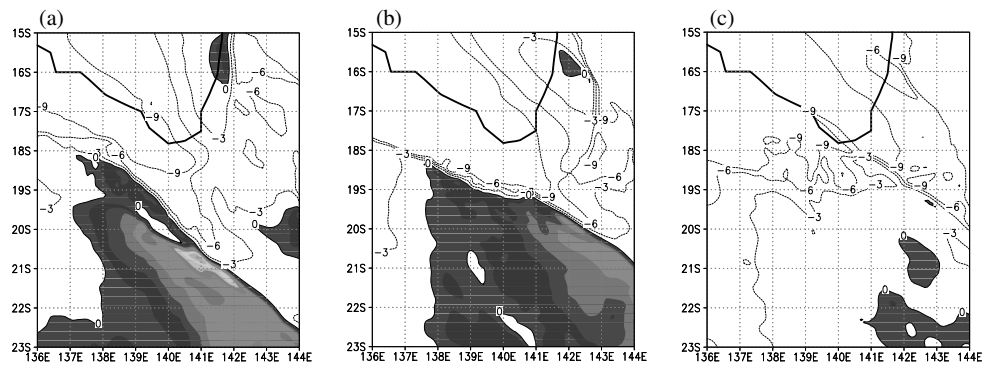

Figure 14. As Fig. 8, but for the relative flow normal to and behind the trough line and the morning-glory disturbance at (a) 1800 EST and (b) 2200 EST and (c) 0000 EST on 28–29 September. Positive values of $u - c$ are shaded and negative contours dotted.

at a height of ∼250 m at selected times. Again u is the wind speed perpendicular to and towards the line in question and c is the propagation speed of that line. (Note that propagation speeds are different for each line.) In these calculations the orientation of the lines, measured anticlockwise from north, is $\sim 60^\circ \pm 1^\circ$ at 1800 EST and $\sim 57^\circ \pm 1^\circ$ at 2200 EST on 28 September and 0000 EST on 29 September. The mean propagation speed of the trough line at 1800 EST on 28 September is ~ 6.1 m s^{-1}. The translation speed of the disturbance corresponding with the morning glory at 2200 EST on 28 September is 10.2 m s^{-1} and at 0000 EST on 29 September it is 12.2 m s^{-1}. The errors in calculating these propagation speeds are estimated to be less than 1 m s^{-1}. It is seen that the relative flow on the southern side of the trough line is positive (i.e. towards the line) before the collision with the south-coast sea breeze. As noted in section 3(a), a positive value of $u - c$ is indicative of a gravity current, while a negative value is characteristic of a bore-like disturbance. Figure 14 shows that $u - c$ becomes negative behind the northward-moving line that emerges from the collision of the northward-moving convergence line

and the sea breeze. After about 0000 EST on 29 September, the relative flow behind the morning glory is everywhere negative and its transition to a bore wave is complete.

4. Conclusions

With a horizontal resolution of 3 km in the finest domain and a commensurate vertical resolution, MM5 in the present configuration has considerable skill in predicting the convergence lines observed in the two GLEX events that we investigated. The higher-resolution and non-hydrostatic formulation allowed a more accurate depiction of the lines than the operational mesoLAPS forecasts in previous studies. MM5 was able to distinguish clearly between the convergence lines corresponding to the north-easterly morning glory and NACL, showing that the former developed out of the east-coast sea-breeze front on Cape York Peninsula south of about 14°S, while the latter formed from the same sea-breeze front to the north of this latitude. Calculations of the low-level flow towards each of these lines showed that both had the character of a gravity current (with the relative flow behind the line and normal to it being positive) during the afternoon and evening, but the morning-glory convergence line progressively acquired the character of a bore as the region of positive relative flow behind it declined overnight. Eventually the region of positive relative flow disappeared, completing the transition to a bore. In contrast, the line marking the NACL retained a gravity-current-like structure. Also, MM5 captured the generation of a bore-like disturbance moving ahead of and separating from the air-mass change in the event of 28–29 September.

Despite its accuracy in representing the 4 October north-easterly disturbances, the model failed to capture a disturbance corresponding to the observed southerly morning glory on this day, but it did predict a northward-moving convergence line about 150 km to the south. This line did not reach the southern gulf coast before the recommencement of daytime mixing, which would have removed the low-level stable layer required for propagation of the shallow disturbance. This failure probably resided in an inaccurate location of the convergence line over the data-sparse region south of the gulf in the initial analysis. These lines formed along the northern perimeter of a ridge from an anticyclone as the latter moved eastwards across the continent.

The calculations support a recently proposed conceptual model for the generation of southerly morning glories in which ageostrophic low-level convergence leads to the formation of a shallow northward-moving cold front in the evening on the southern side of the inland trough. This front collides with an even shallower sea-breeze flow from the southern gulf coast and leads to the formation of a bore-like disturbance that moves northwards on the stable layer provided by the sea-breeze air. Vertical cross-sections of moisture on days with southerly disturbances show a strong meridional gradient in moisture on the northern side of the inland trough. This moisture gradient corresponds to the dry line, which marks the maximum inland penetration of the sea breeze south of the gulf.

Acknowledgements

We are grateful to the ECMWF for providing analysis data. Financial support for the GLEX was provided by the German Research Council (Deutsche Forschungsgemeinschaft). The first author gratefully acknowledges receipt of a research scholarship from the University of Munich, which supported this study, as well as a Rupert Ford Travel Award from the Royal Meteorological Society, which enabled him to visit research facilities in Australia, where part of this work was carried out.

REFERENCES

Clarke, R. H. 1983 Fair-weather nocturnal inland wind surges and atmospheric bores: Part I Nocturnal wind surges. *Aust. Meteorol. Mag.*, **31,** 133–145

1984 Colliding sea breezes and atmospheric bores: Two-dimensional numerical studies. *Aust. Meteorol. Mag.*, **32,** 207–226

Dudhia, J. 1989 Numerical study of convection observed during the winter monsoon experiment using a mesoscale two-dimensional model. *J. Atmos. Sci.*, **46,** 3077–3107

Goler, R. A. and Reeder, M. J. 2004 The generation of the morning glory. *J. Atmos. Sci.*, **61,** 1360–1376

Grell, G. A. 1993 Prognostic evaluation of assumptions used by cumulus parameterizations. *Mon. Weather Rev.*, **121,** 764–787

Grell, G. A., Dudhia, J. and Stauffer, D. 1995 'A description of the 5th generation Penn. State/NCAR mesoscale model (MM5)'. Technical Report 398, NCAR, Boulder, USA

Hong, S.-Y. and Pan, H.-L. 1996 Non-local boundary layer vertical diffusion in a medium-range forecast model. *Mon. Weather Rev.*, **124,** 1322–2399

Jackson, G. E., Smith, R. K. and Spengler, T. 2002 The prediction of low-level mesoscale convergence lines over north-eastern Australia. *Aust. Meteorol. Mag.*, **51,** 13–23

Noonan, J. A. and Smith, R. K. 1986 Sea-breeze circulations over Cape York peninsula and the generation of Gulf of Carpentaria cloud-line disturbances. *J. Atmos. Sci.*, **43,** 1679–1693

1987 The generation of North Australian cloud lines and the 'morning glory'. *Aust. Meteorol. Mag.*, **35,** 31–45

Puri, K., Dietachmayer, G. S., Mills, G. A., Davidson, N. E., Bowen, R. A. and Logan, L. W. 1998 The new BMRC Limited-Area Prediction System LAPS. *Aust. Meteorol. Mag.*, **47,** 203–223

Reeder, M. J. and Smith, R. K. 1998 Mesoscale meteorology. Chapter 5 in *Meteorology of the Southern Hemisphere*, Eds. D. J. Karoly and D. Vincent, American Meteorol. Soc. Monograph 49, Boston, USA

Simpson, J. E. 1997 *Gravity currents in the environment and in the laboratory*. (2nd ed.) Cambridge University Press, UK

Smith, R. K. and Noonan, J. A. 1998 On the generation of low-level mesoscale convergence lines over north-eastern Australia. *Mon. Weather Rev.*, **126,** 167–185

Smith, R. K. and Page, M. A. 1985 Morning glory wind surges and the Gulf of Carpentaria cloud line of 25–26 October 1984. *Aust. Meteorol. Mag.*, **33,** 185–194

Smith, R. K., Crook, N. A. and Roff, G. 1982 Morning Glory: an extraordinary atmospheric undular bore. *Q. J. R. Meteorol. Soc.*, **108,** 937–956

Smith, R. K., Coughlan, M. J. and Lopez, J.-L. 1986 Southerly nocturnal wind surges and bores in north-eastern Australia. *Mon. Weather Rev.*, **114,** 1501–1518

Smith, R. K., Reeder, M. J., Tapper, N. J. and Christie, D. R. 1995 Central Australian cold fronts. *Mon. Weather Rev.*, **123,** 16–38